Applied Mathematics and Physics, 2013, Vol. 1, No. 2, 31-38
Available online at http://pubs.sciepub.com/amp/1/2/3

DOI:10.12691/amp-1-2-3

Hall Effects on the Unsteady Incompressible MHD Fluid Flow with Slip Conditions and Porous Walls

H. Zaman*

Department of Mathematics, Islamia College Chartered University, Peshawar, Pakistan
*Corresponding author: haiderzaman67@yahoo.com

Received June 28, 2013; Revised July 20, 2013; Accepted July 29, 2013

Abstract This work is concerned with the influence of Hall current on unsteady incompressible MHD fluid with slip conditions. The effects of Hall current on uniform suction or injection are also seen. As a special case of this problem for no slip condition, the effects of Hall current on Couette flow are discussed. The resulting unsteady problems for velocity are solved by means of Laplace transform, however, the inversion procedure for obtaining the solution is not a trivial matter. The characteristics of the complex transient velocity, complex overall transient velocity, complex steady state velocity are analyzed and discussed for both the cases. Graphical results for the Hall parameter reveal that it has significant influence on the real and imaginary parts of the velocity profiles.

Keywords: *hall effects, unsteady, Laplace transform, transient velocity, wall slip, porous walls*

Cite This Article: H. Zaman, "Hall Effects On The Unsteady Incompressible MHD Fluid Flow With Slip Conditions and Porous Walls" *Applied Mathematics and Physics* 1, no. 2 (2013): 31-38. doi: 10.12691/amp-1-2-3.

1. Introduction

The study of Hall current is very important in the presence of a magnetic field [1] A current induced in a direction normal to the electric and magnetic fields is called Hall current. Magnetohydrodynamic (MHD) flows with Hall effect are encountered in power generators, MHD accelerators, refrigeration coils, electric transformers etc. Considerable efforts have been devoted to study the effects of Hall current in various directions. The effect of Hall current on the MHD boundary layer flow is considered by authors [2-13]. Furthermore, the heat transfer and Hall effect in the stretching flow are examined in the Refs. [14-20]. Exact solutions of Navier - Stokes equations are rare due to their inherent nonlinearity. Exact solutions are important because they serve as accuracy checks for numerical solutions. Complete integration of these equations is done by computer techniques, but the accuracy of the results can be established only by comparison with exact solutions. In the literature, there are a large number of Newtonian fluid flows for which exact solutions are possible [21,22,23,24,25] The effects of transverse magnetic field on the flow of an electrically conducting viscous fluid have been studied extensively in view of numerous applications to astrophysical, geophysical and engineering problems [26-31]. If the working fluid contains concentrated suspensions then the wall slip can occur [32]. Khaled and Vafai [23] studied the effect of the slip on Stokes and Couette flows due to an oscillating wall.

However, the literature lacks studies that take into account the possibility of fluid slippage at the walls. Applications of these problems appear in microchannels or nanochannels and in applications where a thin film of light oil is attached to the moving plates or when the surface is coated with special coating such as a thick monolayer of hydrophobic octadecyltrichlorosilane [33]. Yu and Ameel [34] imposed non-linear slip boundary conditions on flow in rectangular microchannels.

In this study, the effects of Hall current on the flow of an incompressible, unsteady, viscous, MHD fluid with slip conditions are considered. Unsteady and steady velocity profiles with mass transfer are presented and solved exactly. There is mass injection from one plate and the same amount of suction on the other plate. When the fluid motion is set up from rest, the velocity field contains transients, determined by the initial conditions which gradually disappeared in time. The effects of Hall current and time on the transient velocity and on overall transient velocity has been seen graphically for injection / suction both. The effect of slip parameter on steady state velocity for injection / suction is also shown graphically in the presence of Hall effects. As a limiting case by taking slip parameter $\lambda \to 0$, the effects of Hall parameter on overall transient velocity for Couette flow problem are also discussed in detail.

2. Theoretical Derivation

Consider an MHD incompressible, viscous, unsteady flow problem with Hall effects, in which there is slip between the bottom wall and fluid and also between top wall and fluid. There is mass injection velocity v_W at the bottom wall and mass suction velocity v_W at the top wall, $v_W > 0$ correspond to injection and $v_W < 0$ correspond to suction.

The governing equation for this problem can be obtained as

$$\frac{\partial u(y,t)}{\partial t}+v_w\frac{\partial u(y,t)}{\partial y}=\nu\frac{\partial^2 u(y,t)}{\partial y^2}-\frac{N(1+i\varphi)}{\left(1+\varphi^2\right)}\,u(y,t), \quad (1)$$

where $\nu=\mu/\rho$, $N=\sigma\,B_0^2/\rho$, μ is the dynamic viscosity, ν is the kinematic viscosity, ρ is the density of the fluid, σ is the electric conductivity of the fluid, B_0 is the applied magnetic field, N is the MHD factor or parameter, φ is the Hall parameter. For the boundary conditions we consider the existence of slip between the velocity of the fluid at the walls and speed of the walls.

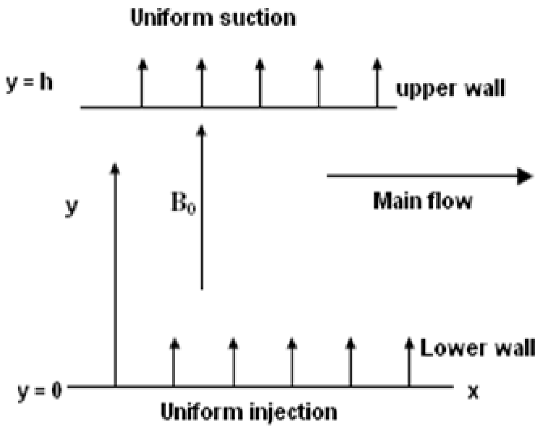

Figure 1. Geometry of the problem

$$u(0,t)-\lambda\left.\frac{\partial u(y,t)}{\partial y}\right|_{y=0}=0 \quad (2)$$

$$u(h,t)+\lambda\left.\frac{\partial u(y,t)}{\partial y}\right|_{y=h}=U_0 \quad (3)$$

The initial condition is

$$u(y,0)=0 \quad (4)$$

where bottom wall is located at $y=0$, top wall is located at $y=h$, λ is the slip parameter, ($\lambda=0$ gives the usual no slip condition at the wall) and U_0 is the velocity at the upper wall. Eqs. (1), (2), (3) and (4) can be non-dimensionalized by defining

$$U=\frac{u}{U_0},\quad Y=\frac{y}{h},\quad \text{and}\quad T=\frac{t}{\tau_c}=\frac{t\ \nu}{h^2}$$

Then Eqs. (1), (2), (3) and (4) become

$$\frac{\partial U(Y,T)}{\partial T}+R_e\,\frac{\partial U(Y,T)}{\partial Y}=\frac{\partial^2 U(Y,T)}{\partial Y^2}-\overline{M}\,U(Y,T) \quad (5)$$

$$U(0,T)-\bar\lambda\left.\frac{\partial U(Y,T)}{\partial Y}\right|_{Y=0}=0 \quad (6)$$

$$U(1,T)+\bar\lambda\left.\frac{\partial U(Y,T)}{\partial Y}\right|_{Y=1}=1 \quad (7)$$

$$U(Y,0)=0 \quad (8)$$

where $\overline{M}=\overline{N}(1+i\varphi)/\left(1+\varphi^2\right)$, $\overline{N}=Nh^2/\nu$, $\bar\lambda=\lambda/h$ and $R_e=v_w\ h/\nu$ (Reynolds number). Decomposing $U(Y,T)$ into two parts say transient part and a steady state part,

$$U(Y,T)=U_t(Y,T)+U_S(Y) \quad (9)$$

Then we have two separate problems and the steady state part will be

$$R_e\,\frac{dU_S(Y)}{dY}=\frac{d^2U_S(Y)}{dY^2}-\overline{M}\,U_S(Y), \quad (10)$$

$$U_S(0)-\bar\lambda\left.\frac{\partial U_S(Y)}{\partial Y}\right|_{Y=0}=0, \quad (11)$$

$$U_S(1)+\bar\lambda\left.\frac{\partial U_S(Y)}{\partial Y}\right|_{Y=1}=1. \quad (12)$$

The solution of Eq. (10) with BCs (11) and (12) can be obtained as

$$U_S(Y)=\frac{e^{aY}\left[\left(1-\bar\lambda a\right)\sinh\left(b_1Y\right)+\bar\lambda b_1\cosh\left(b_1Y\right)\right]}{e^{a}\left[\left(1-\bar\lambda^2\left(a^2-b_1^2\right)\right)\sinh\left(b_1\right)+2\,\bar\lambda b_1\cosh\left(b_1\right)\right]} \quad (13)$$

where $a=R_e/2$ and $b_1=\sqrt{\frac{R_e^2}{4}+\overline{M}}$

If there is no mass transfer at the walls then $R_e=0$, so $a=0$ and $b_1=\sqrt{\overline{M}}=\sqrt{\frac{\overline{N}(1+i\varphi)}{\left(1+\varphi^2\right)}}$, Eq. (13) becomes

$$U_S(Y)=\frac{\sinh\left(\sqrt{\frac{\overline{N}(1+i\varphi)}{\left(1+\varphi^2\right)}}Y\right)+\bar\lambda\sqrt{\frac{\overline{N}(1+i\varphi)}{\left(1+\varphi^2\right)}}\cosh\left(\sqrt{\frac{\overline{N}(1+i\varphi)}{\left(1+\varphi^2\right)}}Y\right)}{\left(1+\bar\lambda^2\frac{\overline{N}(1+i\varphi)}{\left(1+\varphi^2\right)}\right)\sinh\left(\sqrt{\frac{\overline{N}(1+i\varphi)}{\left(1+\varphi^2\right)}}\right)+2\,\bar\lambda\sqrt{\frac{\overline{N}(1+i\varphi)}{\left(1+\varphi^2\right)}}\cosh\left(\sqrt{\frac{\overline{N}(1+i\varphi)}{\left(1+\varphi^2\right)}}\right)}. \quad (14)$$

The transient part problem becomes

$$\frac{\partial U_t(Y,T)}{\partial T}+R_e\,\frac{\partial U_t(Y,T)}{\partial Y}=\frac{\partial^2 U_t(Y,T)}{\partial Y^2}-\overline{M}\,U_t(Y,T) \quad (15)$$

$$U_t(0,T)-\bar\lambda\left.\frac{\partial U_t(Y,T)}{\partial Y}\right|_{Y=0}=0, \quad (16)$$

$$U_t(1,T)+\bar\lambda\left.\frac{\partial U_t(Y,T)}{\partial Y}\right|_{Y=1}=1, \quad (17)$$

$$U_t(Y,0)=-U_S(Y). \quad (18)$$

The solution can be derived by using Laplace transformation techniques [35] . The solution can be shown as

$$U_t(Y,T)=L^{-1}\left[\frac{e^{aY}\left(\left(1-\bar\lambda a\right)\sinh(bY)+\bar\lambda b\cosh(bY)\right)}{e^{a}\,s\left(\left(1-\bar\lambda^2\left(a^2-b^2\right)\right)\sinh(b)+2\,\bar\lambda b\cosh(b)\right)}\right]-U_S(Y) \quad (19)$$

where L^{-1} denotes the inverse Laplace transform, $a=R_e/2$ and $b=\sqrt{\frac{R_e^2}{4}+s+\overline{M}}$. The inverse Laplace transform of above Eq. (19) shows that we have a simple pole at $s=0$ and infinite number of poles (located on the negative real axis) at $s_n = -\left(l_n^2 + a^2 + \overline{M}\right)$, $(n = 1, 2, 3, ...)$, where $l_n = ib_n$, $\left(b_n = \sqrt{\frac{R_e^2}{4} + s_n + \overline{M}}\right)$ and are given by

$$\tan\left(l_n\right) = \frac{-2\overline{\lambda}\, l_n}{1 - \overline{\lambda}^2\left(a^2 + l_n^2\right)}. \tag{20}$$

The transient part velocity becomes

$$\begin{aligned} U_t(Y,T) = &\sum_{n=1}^{\infty} \operatorname{Re} s\left[\overline{U}_t(Y,s)\, e^{sT}\right]_{s=s_n} \\ &+ \sum_{n=1}^{\infty} \operatorname{Re} s\left[\overline{U}_t(Y,s)\, e^{sT}\right]_{s=0} - U_s \end{aligned} \tag{21}$$

where $\operatorname{Re} s$ stands for residue and $\overline{U}_t(Y,s)$ is given by

$$\overline{U}_t(Y,s) = \frac{e^{aY}\left(\left(1-\overline{\lambda}a\right)\ \sinh\left(bY\right) + \overline{\lambda}b\ \cosh\left(bY\right)\right)}{e^{a}\ s\left(\left(1-\overline{\lambda}^2\left(a^2-b^2\right)\right)\ \sinh\left(b\right) + 2\ \overline{\lambda}b\ \cosh\left(b\right)\right)}. \tag{22}$$

We have

$$\sum_{n=1}^{\infty} \operatorname{Re} s\left[\overline{U}_t(Y,s)\, e^{sT}\right]_{s=s_n} = \sum_{n=1}^{\infty} \frac{G_1\left(l_n,Y\right)}{G_2\left(l_n\right)}\, e^{s_nT} \tag{23}$$

Where

$$G_1\left(l_n,Y\right) = e^{aY}\left(\left(1-\overline{\lambda}a\right)\ \sin\left(l_nY\right) + \overline{\lambda}l_n\ \cos\left(l_nY\right)\right), \tag{24}$$

$$G_2\left(l_n\right) = e^{a}\ s_n\left(\overline{\lambda}\left(\overline{\lambda}+1\right)\ \sin\left(l_n\right) - \left(1+2\ \overline{\lambda} - \overline{\lambda}^2\left(a^2+l_n^2\right)\right)\ \frac{\cos\left(l_n\right)}{2l_n}\right). \tag{25}$$

The residue at $s = 0$ gives steady velocity.

$$\sum_{n=1}^{\infty} \operatorname{Re} s\left[\overline{U}_t(Y,s)\, e^{sT}\right]_{s=0} = U_s. \tag{26}$$

The transient part velocity from Eq. (21) becomes

$$\begin{aligned} U_t(Y,T) &= \sum_{n=1}^{\infty} \frac{G_1\left(l_n,Y\right)}{G_2\left(l_n\right)}\, e^{s_nT}, U_t(Y,T) \\ &= \sum_{n=1}^{\infty}\left[\frac{e^{aY}\left(\left(1-\overline{\lambda}a\right)\ \sin\left(l_nY\right) + \overline{\lambda}l_n\ \cos\left(l_nY\right)\right)}{e^{a}\ s_n\left(\overline{\lambda}\left(\overline{\lambda}+1\right)\ \sin\left(l_n\right) - \left(1+2\ \overline{\lambda} - \overline{\lambda}^2\left(a^2+l_n^2\right)\right)\ \frac{\cos(l_n)}{2l_n}\right)} e^{s_nT}\right]. \end{aligned} \tag{27}$$

Therefore, the overall transient solution from Eq. (9) becomes

$$\begin{aligned} U(Y,T) = &\sum_{n=1}^{\infty}\left\{\frac{e^{aY}\left(\left(1-\overline{\lambda}a\right)\ \sin\left(l_nY\right) + \overline{\lambda}l_n\ \cos\left(l_nY\right)\right)}{e^{a}\ s_n\left(\overline{\lambda}\left(\overline{\lambda}+1\right)\ \sin\left(l_n\right) - \left(1+2\ \overline{\lambda} - \overline{\lambda}^2\left(a^2+l_n^2\right)\right)\ \frac{\cos(l_n)}{2l_n}\right)} e^{s_nT}\right\} \\ &+ \frac{e^{aY}\left[\left(1-\overline{\lambda}a\right)\ \sinh\left(b_1Y\right) + \overline{\lambda}b_1\ \cosh\left(b_1Y\right)\right]}{e^{a}\left[\left(1-\overline{\lambda}^2\left(a^2-b_1^2\right)\right)\ \sinh\left(b_1\right) + 2\ \overline{\lambda}b_1\ \cosh\left(b_1\right)\right]}. \end{aligned} \tag{28}$$

2.1. No Slip Problem

When there is no slip $\left(\lambda = 0\right)$ between the fluid and the wall than above problem reduces to

$$\frac{\partial u(y,t)}{\partial t} + v_w\frac{\partial u(y,t)}{\partial y} = \nu\frac{\partial^2 u(y,t)}{\partial y^2} - \frac{N\left(1+i\varphi\right)}{\left(1+\varphi^2\right)}\ u(y,t), \tag{29}$$

$$u(0,t) = 0,\ u(h,t) = U_0,\ u(y,0) = 0. \tag{30}$$

This is an unsteady MHD incompressible viscous Couette flow problem with Hall effects, in which the bottom wall is fixed and subjected to a mass injection velocity v_w, and there is mass suction velocity v_w at the top wall. The top plate is stationary when $t < 0$, there is only mass transfer in the transverse direction, say $y-$ direction. At $t = 0$, the top wall is started impulsively to a constant velocity U_0. The solution of this problem can be derived from above problem by applying no slip condition $\overline{\lambda} = 0$. Steady state velocity can be deduced from Eq. (13) by putting $\overline{\lambda} = 0$.

$$U_s(Y) = \frac{e^{aY}\sinh\left(b_1Y\right)}{e^{a}\sinh\left(b_1\right)}, \tag{31}$$

where $a = R_e / 2$ and $b_1 = \sqrt{\frac{R_e^2}{4} + \overline{M}}$.

If there is no mass transfer at the walls then $R_e = 0$, so $a = 0$ and $b_1 = \sqrt{\overline{M}} = \sqrt{\frac{\overline{N}(1+i\varphi)}{\left(1+\varphi^2\right)}}$, Eq. (31) becomes

$$U_s(Y) = \frac{\sinh\left(\sqrt{\frac{\overline{N}(1+i\varphi)}{\left(1+\varphi^2\right)}}Y\right)}{\sinh\left(\sqrt{\frac{\overline{N}(1+i\varphi)}{\left(1+\varphi^2\right)}}\right)}. \tag{32}$$

The transient part solution can be obtained from Eq. (27) by putting $\overline{\lambda} = 0$.

$$U_t(Y,T) = U_t(Y,T) = -\sum_{n=1}^{\infty}\left[\frac{e^{aY}\sin\left(l_nY\right)}{e^{a}\ s_n\ \frac{\cos(l_n)}{2l_n}}e^{s_nT}\right], \tag{33}$$

The overall transient solution can be deduced from Eq. (28) by putting $\overline{\lambda} = 0$.

$$U(Y,T) = -\sum_{n=1}^{\infty}\left\{\frac{e^{aY}\sin\left(l_nY\right)}{e^{a}\ s_n\ \frac{\cos(l_n)}{2l_n}}e^{s_nT}\right\} + \frac{e^{aY}\sinh\left(b_1Y\right)}{e^{a}\sinh\left(b_1\right)}. \tag{34}$$

where $a = R_e / 2$, $b_1 = \sqrt{\frac{R_e^2}{4} + \overline{M}}$, $l_n = n\pi$, $s_n = -\left(n^2\pi^2 + \frac{R_e^2}{4} + \overline{M}\right)$. The Eq. (34) can be written as

$$\begin{aligned} U(Y,T) = &\frac{2\pi e^{-\left(\frac{R_e^2}{4}+\overline{M}\right)} e^{\frac{R_e}{2}Y}}{e^{\frac{R_e}{2}}}\sum_{n=1}^{\infty}\left\{\frac{n(-1)^n\sin\left(n\pi Y\right)e^{-n^2\pi^2T}}{\left(n^2\pi^2 + \frac{R_e^2}{4} + \overline{M}\right)}\right\} \\ &+ \frac{e^{\frac{R_e}{2}Y}\sinh\left(\sqrt{\frac{R_e^2}{4} + \overline{M}}Y\right)}{e^{\frac{R_e}{2}}\sinh\left(\sqrt{\frac{R_e^2}{4} + \overline{M}}\right)}. \end{aligned} \tag{35}$$

where $\overline{M} = \overline{N}\left(1+i\varphi\right)/\left(1+\varphi^2\right)$.

3. Graphs and Discussion

In this part we discuss the variation of the real and imaginary parts of the complex transient part velocity U_t, complex overall transient velocity U, complex steady state velocity U_s with distance from the wall Y for different values of Reynolds number R_e, Hall parameter φ, magnetic field parameter $\overline{N}$, slip parameter $\overline{\lambda}$ and time T. Figure 2 and figure 3 hows the variation of real and imaginary parts of the transient part velocity U_t with distance from the wall Y for several values of Hall parameter φ by keeping $\overline{N}$, $\overline{\lambda}$ and T fixed. Figure 2 shows that when there is mass suction $R_e < 0$ at the top wall, with increase in Hall parameter, the real part of the transient part velocity increases in magnitude. Figure 3 shows that when there is mass suction $R_e < 0$ at the top wall, with increase in Hall parameter, the imaginary part of the transient part velocity also decreases in magnitude. Figure 4 shows that when there is mass injection $R_e > 0$ at the bottom wall, with increase in Hall parameter, the real part of the transient part velocity U_t increases. Figure 5 shows that when there is mass injection $R_e > 0$ at the bottom wall, with increase in Hall parameter, the imaginary part of the transient part velocity U_t decreases and will become weaker as compared to the case of real. From Figure 6 it is observed that for suction at top wall and for fixed values of $\overline{\lambda}$, φ and $\overline{N}$, the real part of the transient part velocity U_t decreases in magnitude with increase in time. From Figure 7 it is observed that for suction at top wall and for fixed values of $\overline{\lambda}$, φ and $\overline{N}$, the imaginary part of the transient part velocity U_t also decreases in magnitude with increase in time and will become weaker as compared to the case of real. From Figure 6 and Figure 7 it is seen that the real and imaginary parts of the transient part velocity will decay with time, which is consistent with what we expected.

Figure 8 shows that for injection at bottom wall and for fixed values of $\overline{\lambda}$, $\overline{N}$ and φ the real part of the transient part velocity U_t decreases in magnitude with increase in time. Figure 9 shows that for injection at bottom wall and for fixed values of $\overline{\lambda}$, $\overline{N}$ and φ the imaginary part of the transient part velocity U_t decreases in magnitude with increase in time. From Figure 8 and Figure 9 it is seen that the real and imaginary parts of the transient part velocity will decay with time. From Figure 6, Figure 7 Figure 8 and Figure 9 it is clear that after a certain time, the complex transient part velocity will die away and velocity will become developed. Figure 10 and Figure 11 indicates variation of the real and imaginary parts of overall transient velocity U with Y for fixed values of $\overline{\lambda}$, $\overline{N}$ and T. Figure 10 shows that for $R_e = -5 < 0$, with increase in Hall parameter φ, real part of the overall transient velocity U increases. Figure 11 shows that for $R_e = -5 < 0$, with increase in Hall parameter φ, imaginary part of the overall transient velocity U decreases. Figure 12 shows that for $R_e = 5 > 0$, with increase in Hall parameter φ, the real part of the overall transient velocity U increases. Figure 13 shows that for $R_e = 5 > 0$, with increase in Hall parameter φ, the imaginary part of the overall transient velocity U decreases. The real and imaginary parts of the overall transient velocities for $R_e = 5$ at different times are depicted in Figure 14 and Figure 15. Figure 14 shows that for mass injection at the bottom wall, real part of the overall transient velocity U increases with increase in time. Figure 15 shows that for mass injection at the bottom wall, imaginary part of the overall transient velocity U decreases with increase in time. Figure 16 and Figure 17 illustrates the variation of real and imaginary parts of the steady state velocity U_s with Y for several values of slip parameter $\overline{\lambda}$ and for fixed value of $\overline{N}$ and φ. Figure 16 shows that for suction at the top wall with increase in slip parameter $\overline{\lambda}$, the real part of the steady state velocity U_s increases. Figure 17 shows that for suction at the top wall with increase in slip parameter $\overline{\lambda}$, the imaginary part of the steady state velocity U_s increases.

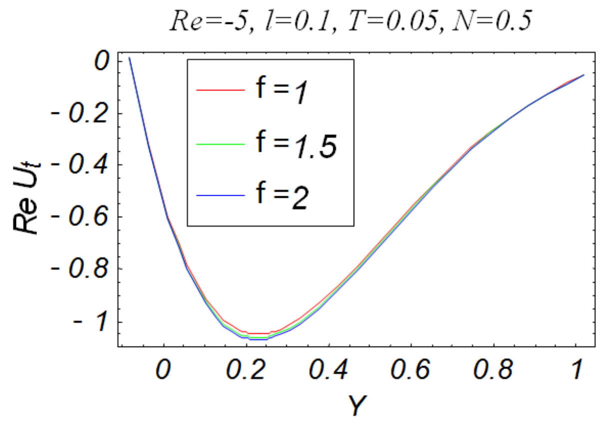

Figure 2. Variation of Re[U_t] with Y for several values of φ and $R_e = -5$

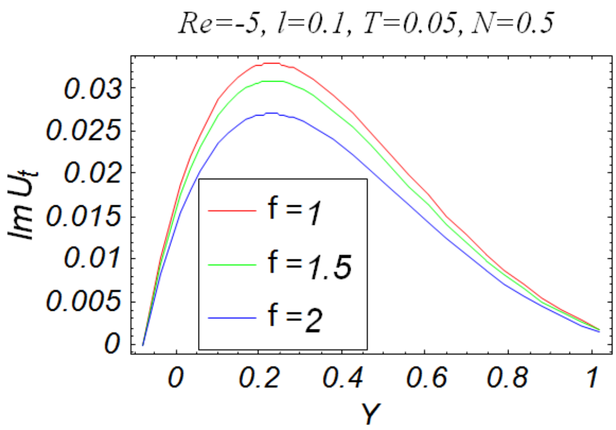

Figure 3. Variation of Im[U_t] with Y for several values of φ and $R_e = -5$

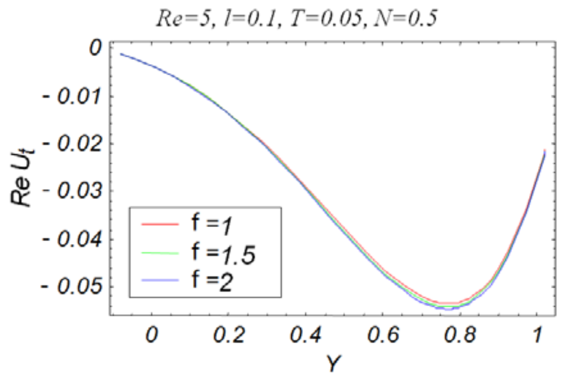

Figure 4. Variation of Re[U_t] with Y for several values of φ and $R_e = 5$

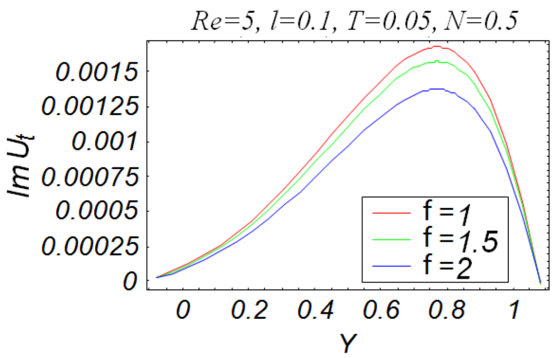

Figure 5. Variation of Im[U_t] with Y for several values of φ and $R_e = 5$

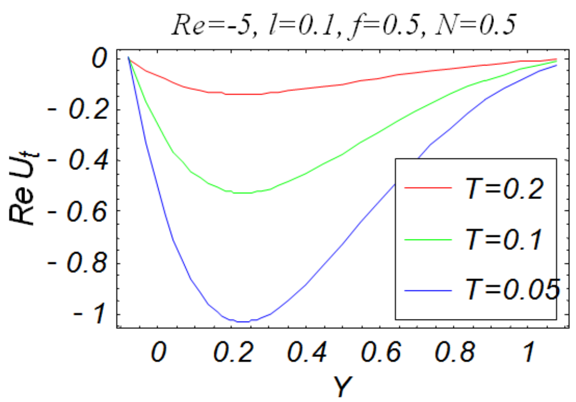

Figure 6. Variation of Re[U_t] with Y for several values of T and $R_e = -5$

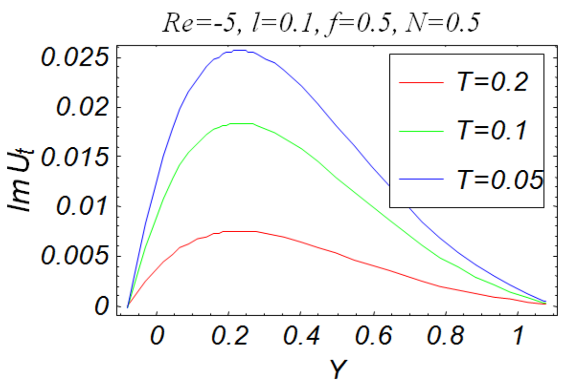

Figure 7. Variation of Im[U_t] with Y for several values of T and $R_e = -5$

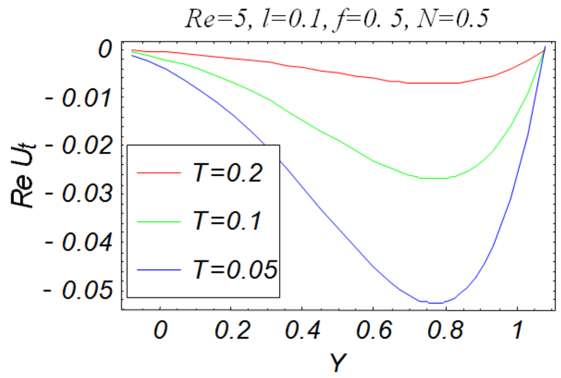

Figure 8. Variation of Re[U_t] with Y for several values of T and $R_e = 5$

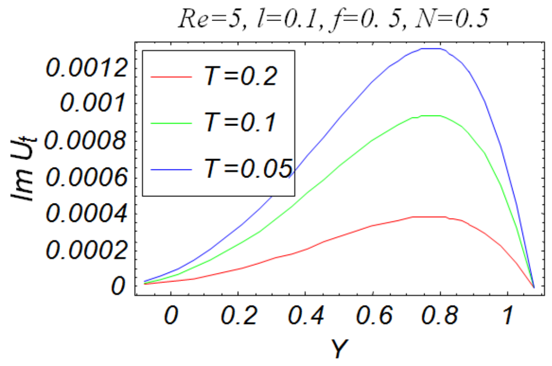

Figure 9. Variation of Im[U_t] with Y for several values of T and $R_e = 5$

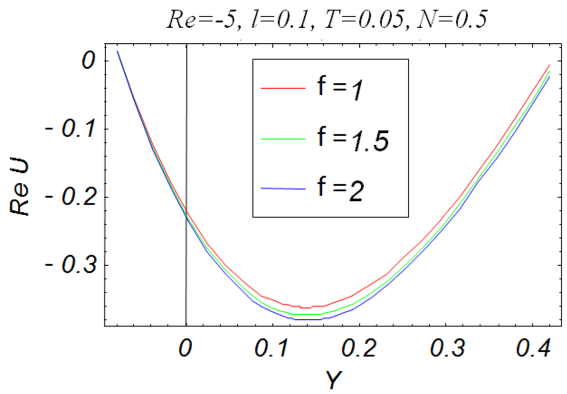

Figure 10. Variation of Re[U_t] with Y for several values of φ and $R_e = -5$

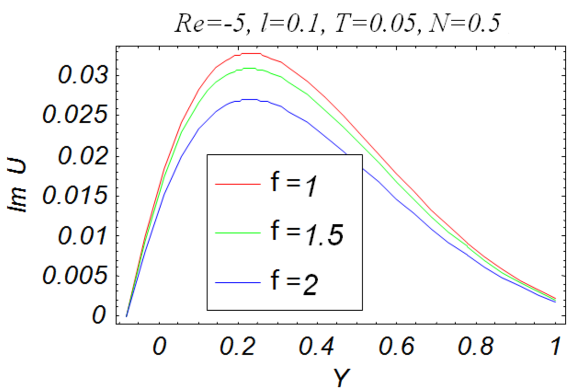

Figure 11. Variation of Im[U_t] with Y for several values of φ and $R_e = -5$

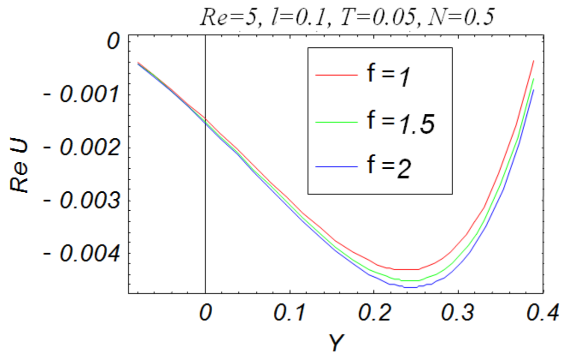

Figure 12. Variation of Re[U_t] with Y for several values of φ and $R_e = 5$

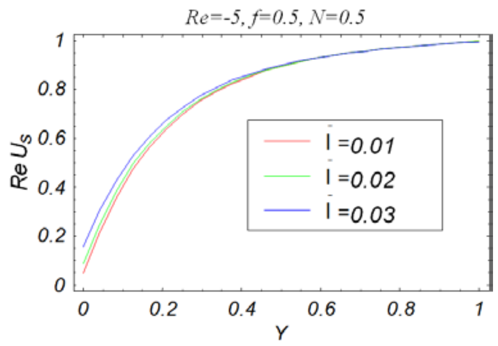

Figure 16. Variation of Re[U_t] with Y for several values of $\bar{\lambda}$ and $R_e = -5$

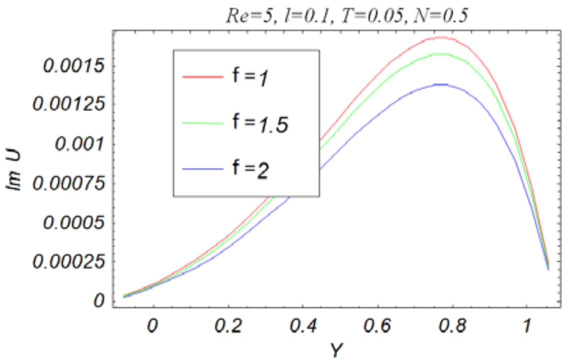

Figure 13. Variation of Im[U_t] with Y for several values of φ and $R_e = 5$

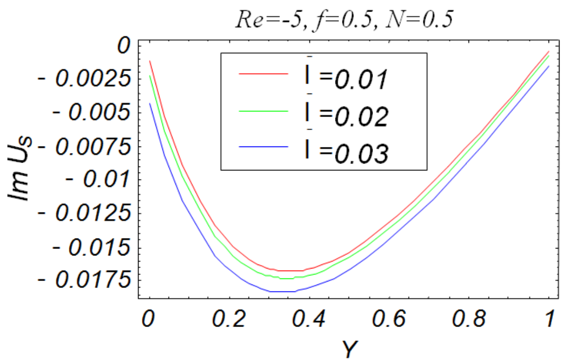

Figure 17. Variation of Im[U_t] with Y for several values of $\bar{\lambda}$ and $R_e = -5$

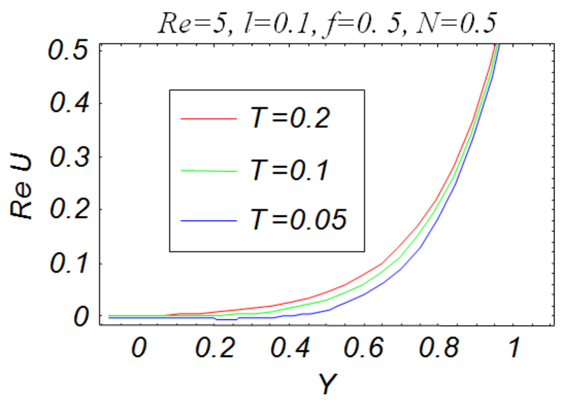

Figure 14. Variation of Re[U_t] with Y for several values of T and $R_e = 5$

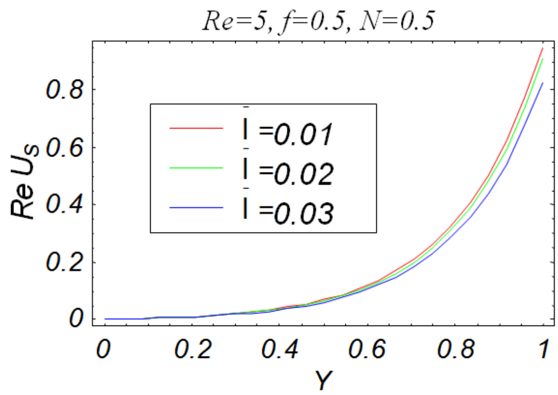

Figure 18. Variation of Re[U_t] with Y for several values of $\bar{\lambda}$ and $R_e = 5$

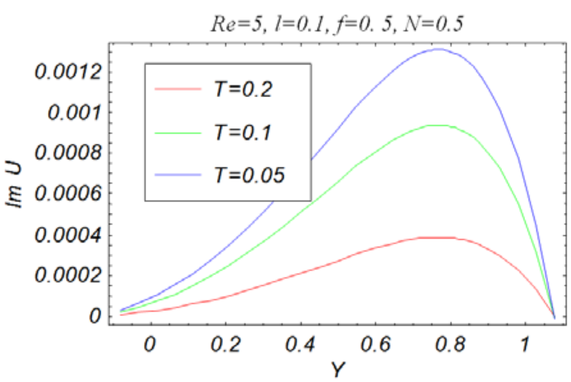

Figure 15. Variation of Im[U_t] with Y for several values of T and $R_e = 5$

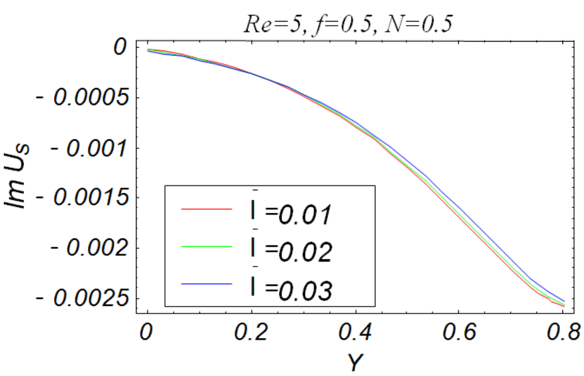

Figure 19. Variation of Im[U_t] with Y for several values of $\bar{\lambda}$ and $R_e = 5$

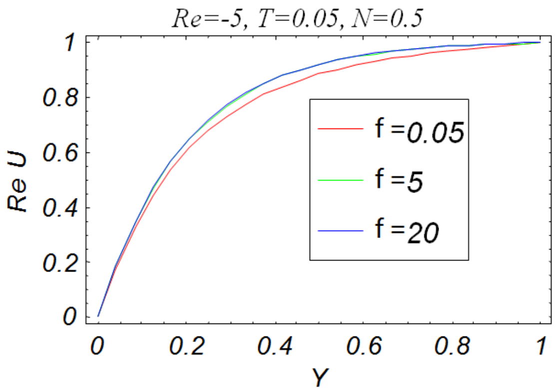

Figure 20. Variation of Re[U] with Y for several values of φ and $R_e = -5$ for Couette flow.

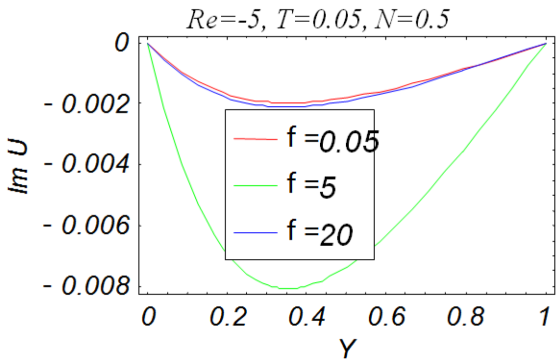

Figure 21. Variation of Im[U] with Y for several values of φ and $R_e = -5$ for Couette flow.

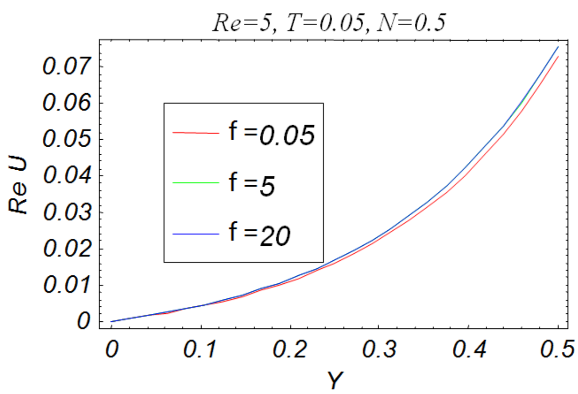

Figure 22. Variation of Re[U] with Y for several values of φ and $R_e = 5$ for Couette flow.

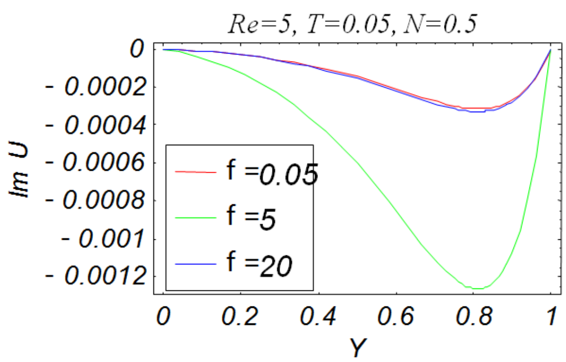

Figure 23. Variation of Im[U] with Y for several values of φ and $R_e = 5$ for Couette flow.

Figure 18 shows that for injection at the bottom wall with increase in slip parameter $\bar{\lambda}$, the real part of the steady state velocity U_S decreases. Figure 19 shows that for injection at the bottom wall with increase in slip parameter $\bar{\lambda}$, the imaginary part of the steady state velocity U_S increases. Figure 20, Figure 21, Figure 22 and Figure 23 are plotted for Hall current on Couette flow with no slip. Figure 20 and Figure 21 indicates variation of the real and imaginary parts of overall transient velocity U with Y for fixed values of $\bar{N}$ and T . Figure 20 shows that for $R_e = -5 < 0$, with increase in Hall parameter φ, real part of the overall transient velocity U increases. Fig 21. shows that for $R_e = -5 < 0$, with increase in Hall parameter φ , imaginary part of the overall transient velocity U increases. Figure 22 shows that for $R_e = -5 > 0$, with increase in Hall parameter φ, the real part of the overall transient velocity U increases. Figure 23 shows that for $R_e = -5 > 0$, with increase in Hall parameter φ , the imaginary part of the overall transient velocity U decreases.

4. Final Remarks

In this study exact solutions for the velocity field in the presence of Hall current, magnetic field, porosity and slip parameter are constructed. A uniform magnetic field is applied transversely to the flow. The exact solutions of the velocity field for flow subjected to the slip conditions between the two parallel plates and fluid are obtained by means of Laplace transform. The solutions so obtained, depending on the initial and the boundary conditions, are presented as sum of the steady state transient solutions. The results for Couette flow with Hall effects are also found by taking $\bar{\lambda} = 0$. Graphical results for mass transfer and Hall current reveal that it has significant influence on the velocity distribution. The current analysis will be useful in dealing with real engineering problems.

References

[1] Craner, K. P. and Pai, S. I., Magnetofluid Dynamics for Engineers and Applied Physicists, McGraw-Hill, New York, 1973.

[2] Katagiri, M., The effect of Hall currents on the magnetohydrodynamic boundarylayer flow past a semi-infinite flate plate. J. Phys. Soc. Japan 27 1051-1059 1969.

[3] Gupta, A. S., Hydromagnetic flow past a porous flate plate with Hall effects. Acta Mech. 22 281-287 1975.

[4] Pop, I. and Soundalgekar, V. M., Effects of Hall current on hydromagnetic flow near a porous plate. Acta Mech. 20 315-318 1974.

[5] Debnath, L., Ray, S. C. and Chatterjee, A. K., Effects of Hall current on unsteady hydromagnetic flow past a porous plate in a rotating fluid system. Z. Angew. Math. Mech. 59 469-471 1979.

[6] Hayat, T., Naz, R. and Asghar, S., Hall effects on unsteady duct flow of a non-Newtonian fluid in a porous medium. Appl. Math. Computation 157 103-114 2004.

[7] Sato, H., The Hall effects in the viscous flow of ionized gas between parallel plates under transverse magnetic field. J. Phys. Soc. Japan 16 1427-1433 1961.

[8] M. A. Hossain, Effect of Hall current on unsteady hydromagnetic free convection flow near an infinite vertical porous plate. J. Phys. Soc. Japan 55 2183-2190 1986.

[9] M. A. Hossain, K. Mohammad, Effect of Hall current on hydromagnetic free convection flow near an accelerated porous plate. J. Phys. Soc. Japan 27 1531-1535 1988.

[10] Hossain, M. A., Rashid, R. I. M. A., The effect of Hall currents on hydromagnetic free convection flow near an accelerated porous plate. J. Phys. Soc. Japan 56 97-104 1987.

[11] Raptis, A., Ram, P. C., Effects of Hall current and rotation. Astrophys. Space Sci. 106 257-264 1984.

[12] Ram, P. C., Hall effects on free convection flow and mass transfer through a porous medium. Warme Stoffubertrag 22 223-225 1988

[13] Asghar, S., Mohyuddin, M. R. and Hayat, T., Effects of Hall current and heat transfer on flow due to a pull of ecentric rotating disks. Int. J. Heat and Mass Transfer 48 599-607 2005.

[14] Abo-Eldahab, E. M. and Elbarbary, M. E., Hall current effect on magnetohydrodynamic free convection flow past a semi-infinite vertical plate with mass transfer. Int. J. Eng. Sci. 39 1641-1652 2001.

[15] Abo-Eldahab, E. M. and Abd El Aziz, M., Hall current and Ohmic heating effects on mixed convection boundary layer flow of a micropolar fluid from a rotating cone with power law variation in surface temperature. Int. Comm. Heat Mass Transfer 31 751-762 2004.

[16] Abo-Eldahab, E. M. and Salem, A. M., Hall effects on MHD free convection flow of a non-Newtonian power law fluid at a stretching surface. Int. Comm. Heat Mass Transfer 31 343-354 2004.

[17] Abo-Eldahab, E. M. and Abd El Aziz, M., Flow and heat transfer in a micropolar fluid past a stretching surface embedded in a non-Darcian porous medium with uniform free stream. Appl. Math. Comput. 162 881-899 2005.

[18] Ahmad, M., Zaman, H. and Rehman, N., Effects of Hall current on unsteady MHD flows of a second grade fluid. Cent. Eur. J. Phys. 8(3) 422-431 2010.

[19] Ayub, M., Zaman, H. and Ahmad, M., Series solution of hydromagnetic flow and heat transfer with Hall effect in a second grade fluid over a stretching sheet. Cent. Eur. J. Phys. 8(1) 135-149 2010.

[20] Khan, M., Asghar, S. and Hayat, T., Hall effect on the pipe flow of a Burgers' fluid: An exact solution. Nonlinear Analysis: Real World Applications. 10 974-979 2009.

[21] Fang, T., A note on the incompressible Couette flow with porous walls. Int. Comm. Heat Mass Transfer. 31 (1)31-41 2004.

[22] Schlichting, H. and Gersten, K., *Boundary layer theory*, 8th Edition, Springer-Verlag, Berlin Heidelberg, 2000.

[23] Khaled, A. R. A. and Vafai, K., The effect of the slip condition on Stokes and Couette flows due to an oscillating wall: exact solutions. Int. J. Non-Linear Mech.39 795-809 2004.

[24] Hayat, T., Khan, M., Siddiqui, A. M. and Asghar, S., Transient flows of a second grade fluid. Int. J. Non-Linear Mech. 39 1621-1633 2004.

[25] Erdogan, M. E., A note on an unsteady flow of a viscous fluid due to an oscillating plane wall. Int. J. Non-Linear Mech. 35 1-6 2000.

[26] Hayat, T., Javed, T. and Abbas, Z., MHD flow of a micropolar fluid near a stagnation point towards a non-linear stretching surface. Nonlinear Analysis: Real World Applications. 10 1514-1526 2009.

[27] Hayat, T., Abbas, Z. and Javed, T., MHD stagnation point flow and heat transfer over a permeable surface through a porous space. Journal of Porous media. 12 183-195 2009.

[28] Asghar, S., Khan, M. and Hayat, T., Magnetohydrodynamic transient flows of a non-Newtonian fluid. Int. J. Non-Linear Mech. 40 589-601 2005.

[29] Khan, M., Hyder Ali, S., Hayat, T. and Fetecau, C., MHD flows of a second grade fluid between two side walls perpendicular to a plate through a porous medium. Int. J. Non-Linear Mech. 43 302-319 2008.

[30] Cortell, R., MHD flow and mass transfer of an electrically conducting fluid of second grade in a porous medium over a stretching sheet with chemically reactive pecies. Chem. Eng and Processing. 46 721-728 2007.

[31] Hayat, T., Zaman, H. and Ayub, M., Analytic solution of hydromagnetic flow with Hall effect over a surface stretching with a power law velocity. Numerical Methods for Partial Differential Equations. 27(4) 937-959 2010.

[32] Soltani, F. and Yilmazer, U., Slip velocity and slip layer thickness in flow of concentrated suspensions. J. Appl. Polym. Sin. 70 515-52 1998.

[33] Derek, C., Tretheway, D. C. and Meinhart, C. D., Apparent fluid slip at hydrophobic microchannel walls. Phys. Fluids. 14 9-12 2002.

[34] Yu, S. and Ameel, T. A., Slip-flow Heat Transfer in Rectangular Micro channels. Int. J. Heat and Mass Transfer. 44 4225-4234 2002.

[35] Roberts, G. E. and Kaufman, H., Tables of Laplace Transforms, p. 284, W. B. Saunders Company, Philadelphia 1966.